
Neural Analogical Matching

Maxwell Crouse
 Qualitative Reasoning Group
 Northwestern University
 mvcrouse@u.northwestern.edu

Constantine Nakos
 Qualitative Reasoning Group
 Northwestern University
 cnakos@u.northwestern.edu

Ibrahim Abdelaziz
 IBM Research
 IBM T.J. Watson Research Center
 ibrahim.abdelaziz1@ibm.com

Kenneth Forbus
 Qualitative Reasoning Group
 Northwestern University
 forbus@northwestern.edu

Abstract

Analogy is core to human cognition. It allows us to solve problems based on prior experience, it governs the way we conceptualize new information, and it even influences our visual perception. The importance of analogy to humans has made it an active area of research in the broader field of artificial intelligence, resulting in data-efficient models that learn and reason in human-like ways. While analogy and deep learning have generally been considered independently of one another, the integration of the two lines of research seems like a promising step towards more robust and efficient learning techniques. As part of the first steps towards such an integration, we introduce the Analogical Matching Network; a neural architecture that learns to produce analogies between structured, symbolic representations that are largely consistent with the principles of Structure-Mapping Theory.

1 Introduction

Analogical reasoning is a form of inductive reasoning that cognitive scientists consider to be one of the cornerstones of human intelligence [1, 2, 3]. Analogy shows up at nearly every level of human cognition, from low-level visual processing [4] to abstract conceptual change [5]. Problem solving using analogy is common, with past solutions forming the basis for dealing with new problems [6, 7]. Analogy also facilitates learning and understanding by allowing people to generalize specific situations into increasingly abstract schemas [8].

Many different theories have been proposed for how humans perform analogy [9, 10, 11, 12]. One of the most influential theories is Structure-Mapping Theory (SMT) [11], which posits that analogy involves the alignment of structured representations of objects or situations subject to certain constraints. Key characteristics of SMT are its use of symbolic representations and its emphasis on relational structure, which allow the same principles to apply to a wide variety of domains.

Until now, the symbolic, structured nature of SMT has made it a poor fit for deep learning. The representations produced by deep learning techniques are incompatible with off-the-shelf SMT implementations like the Structure-Mapping Engine (SME) [13], while the symbolic graphs that SMT assumes as input are challenging to encode with traditional neural methods. However, recent advances in deep learning have made it possible to bridge the gap between the two traditions, providing the architectural tools needed to create neural networks that can learn to produce analogies.

Contributions: We introduce the Analogical Matching Network (AMN), a neural architecture that learns to produce analogies between symbolic representations. Though trained on purely synthetic data, we show over a diverse set of existing analogy problems that AMN’s outputs are largely

consistent with SMT. With AMN, we aim to push the boundaries of deep learning and extend them to an important area of human cognition. It is our hope that future generations of neural architectures can reap the same benefits from analogy that symbolic reasoning systems and humans currently do.

2 Related Work

Many different computational models of analogy have been proposed [14, 15, 13], each instantiating a different cognitive theory of analogy. The differences between them are compounded by the computational costs of analogical reasoning, a provably NP-HARD problem [16]. These computational models are often used to test cognitive theories of human behavior; however, we note that they are useful tools for more applied tasks as well. For instance, the computational model we compare to in this work, the Structure-Mapping Engine (SME), has been used in natural language question-answering [17, 18], computer vision [19, 20], and machine reasoning [21, 22].

Many of the early approaches to analogy were connectionist [23]. The STAR architecture of [24] used tensor product representations of structured data to perform simple analogies of the form $R(x, y) \Rightarrow S(f(x), f(y))$; though their method could not operate over higher-order structural inputs. Drama [25] was an implementation of the multi-constraint theory of analogy [12] that employed a holographic representation similar to tensor products to embed structure. While more capable of handling higher-order structure than STAR; Drama had difficulty when dealing with several propositions simultaneously due to the noisiness of its method for composing several distributed representations together. LISA [26, 27] was a hybrid symbolic connectionist approach to analogy. It staged the mapping process temporally, generating mappings from elements of the compared representations that were activated at the same time. Though it modeled many aspects of human reasoning (e.g., working memory limitations), as pointed out in [28], it had trouble when presented with multiple structurally ambiguous mapping possibilities.

The significance of analogical reasoning has been somewhat unrecognized by the deep learning community, with only a few recent deep learning works incorporating cognitive theories of analogy [29, 30]. Generally, prior deep learning work has only considered analogy as solving simple problems of the form $A : B :: C : D$ [31, 32], with the task being to identify a relation holding with some set of examples and then applying that relation to novel data. Still, such prior works demonstrated progress in applying analogy to more natural perceptual data in the form of images or language. As of yet, no work has explored an end-to-end deep-learning approach to analogy that operates over the graph-based symbolic representations used with standard computational models of analogy.

3 Structure-Mapping Theory

In Structure-Mapping Theory (SMT) [11], analogy centers around the structural alignment of *relational representations* (see Figure 1). A relational representation is a set of logical expressions constructed from entities (e.g., sun), attributes (e.g., YELLOW), functions (e.g., TEMPERATURE), and relations (e.g., GREATER). Structural alignment is the process of producing a *mapping* between two relational representations (referred to as the *base* and *target*). A mapping is a triple $\langle M, C, S \rangle$, where M is a set of *correspondences* between the base and target, C is a set of *candidate inferences* (i.e., inferences about the target that can be made from the structure of the base), and S is a *structural evaluation score* that measures the quality of M . Correspondences are pairs of elements between the base and target (i.e., expressions or entities) that are identified as matching with one another. While entities can be matched together irrespective of their labels, there are more rigorous criteria for matching expressions. SMT asserts that matches should satisfy the following properties

1. *One-to-One*: Each element of the base and target can be a part of *at most* one correspondence
2. *Parallel Connectivity*: Two expressions can be in a correspondence with each other only if their arguments are also in a correspondence with each other
3. *Tiered Identicality*: Relations of expressions in a correspondence must match identically, but functions need not be identical if their correspondence would support structural connectivity
4. *Systematicity*: Preference should be given to mappings with more deeply nested expressions

To understand these properties, we will use the example in Figure 1. A match M between the base (solar system) and the target (atom) is a set of correspondences (i.e., pairings) between elements from

[1] nucleus	[8] sun
[2] electron	[9] planet
[3] MASS([1])	[10] MASS([8])
[4] MASS([2])	[11] MASS([9])
[5] ATTRACTS([1], [2])	[12] TEMPERATURE([8])
[6] REVOLVES-AROUND([2], [1])	[13] TEMPERATURE([9])
[7] GREATER([3], [4])	[14] REVOLVES-AROUND([9], [8])
	[15] GREATER([10], [11])
	[16] GREATER([12], [13])
	[17] ATTRACTS([9], [8])
	[18] CAUSES(AND([15], [17]), [14])
	[19] YELLOW([8])

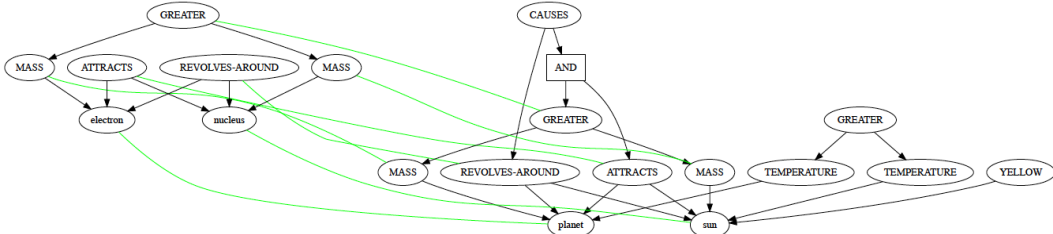


Figure 1: Relational and graph representations for models of the atom (left) and solar system (right). Light green edges indicate the set of correspondences between the two graphs.

both sets, e.g., $\{\langle [1], [8] \rangle, \langle [2], [9] \rangle\}$. The one-to-one constraint restricts each element to be a member of at most one correspondence. Thus, if $\langle [7], [15] \rangle$ was a member of M , then $\langle [7], [16] \rangle$ could not be added to M . Parallel connectivity enforces correspondence between arguments if the parents are in correspondence. In this example, if $\langle [7], [15] \rangle$ was a member of M , then both $\langle [3], [10] \rangle$ and $\langle [4], [11] \rangle$ would need to be members of M . In addition, argument order for ordered relations is enforced with parallel connectivity. Tiered identicity is not relevant in this example; however, if [10] used the label WEIGHT instead of MASS, tiered identicity could be used to match [3] and [10], since such a correspondence would allow for a match between their parents. The last property, systematicity, results in larger correspondence sets being preferred over smaller ones. Note that the singleton set $\{\langle [1], [8] \rangle\}$ satisfies SMT’s constraints, however, it is clearly not useful. Systematicity captures the natural preference towards larger, more interesting matches.

Candidate inferences are viewed as structural completion [23, 33, 34], i.e., the process of filling in missing statements in the target from the base around the overlapping structure of the base and target. Given a set of correspondences M , candidate inferences are created from statements in the base that are supported by expressions in M , but which are not a part of M themselves. Going back to our example, if the solar system was considered the base and the atom the target, then a candidate inference could be $CAUSES(AND([7], [5]), [6])$ (i.e., that the electron revolving around the nucleus is caused by the nucleus having greater mass and attracting the electron). In this work, we adopt SME’s default method for computing candidate inferences. Thus, valid candidate inferences are all statements that have *some* dependency that is included in the correspondences or an ancestor that is a candidate inference (e.g., an expression whose parent has arguments in the correspondences).

The concepts above carry over naturally into graph-theoretic concepts. The base and target are considered semi-ordered directed-acyclic graphs (DAGs) $G_B = \langle V_B, E_B \rangle$ and $G_T = \langle V_T, E_T \rangle$, with V_B and V_T being sets of nodes and E_B and E_T being sets of edges. Each node corresponds to some expression in the base or target and has a label given by its relation, function, attribute, or entity name. Associated with each node is a set of edges that connect it to its immediate arguments. Each edge is an ordered pair of vertices of the form $e_{ij} = \langle v_i, v_j \rangle$, with v_i being the parent and v_j being the argument. Structural alignment is the process of finding a maximum weight bipartite matching $M \subseteq V_B \times V_T$, where correspondences are tuples $\langle b_i, t_j \rangle \in M$ and M satisfies the pairwise-disjunctive constraints imposed by parallel connectivity. Finding candidate inferences is the process of determining the subset of nodes from $V_B \setminus \{b_i : \langle b_i, t_j \rangle \in M\}$ with support in M .

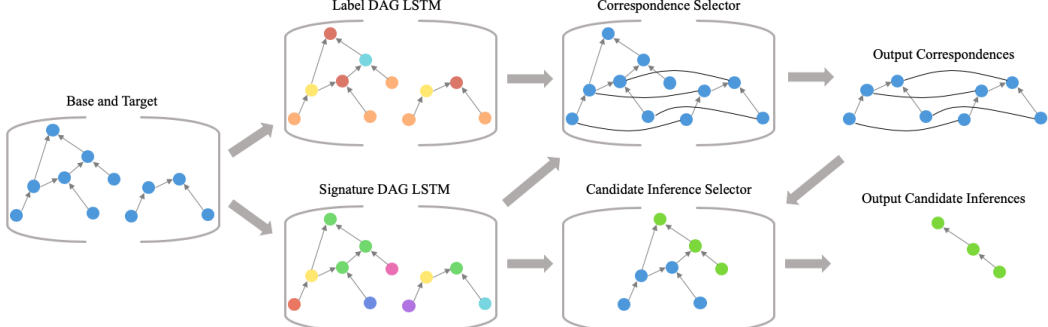


Figure 2: An overview of the model pipeline

4 Model

4.1 Model Components

Given a base $G_B = \langle V_B, E_B \rangle$ and target $G_T = \langle V_T, E_T \rangle$, AMN produces a set of correspondences $M \in V_B \times V_T$ and a set of candidate inferences $I \in V_B \setminus \{b_i : \langle b_i, t_j \rangle \in M\}$. A key design choice of this work was to avoid using rules or architectures that force particular outputs when possible. AMN is *not* forced to output correspondences that satisfy the constraints of SMT; instead, conformance with SMT is reinforced through performance on training data. Our architecture is Transformer-based [35] and draws heavily upon both pointer networks [36] and the work of [37]. A high-level overview is given in Figure 2, which shows how each of the three main components (graph embedding, correspondence selection, and candidate inference selection) interact with one another.

Representing Structure: When embedding the nodes of G_B and G_T , there are representational concerns to keep in mind. First, because matching should be done on the basis of structure, the labels of entities should not be taken into account during the alignment process. Second, because SMT’s constraints require AMN to be able to recognize when a particular node is part of multiple correspondences, AMN should maintain distinguishable representations for distinct nodes, even if those nodes have the same labels. Last, the architecture should not be vocabulary dependent, i.e., AMN should generalize to symbols it has never seen before. To achieve each of these, AMN first parses the original input into two separate graphs, a *label graph* and a *signature graph* (see Figure 3).

The label graph is used to get an estimate of the structural similarity of two expressions. To generate the label graph, AMN first substitutes each entity node’s label with a generic entity token. This reflects the fact that entity labels have no inherent utility for producing matchings. Then, each function and predicate node is assigned a randomly chosen generic label (from a fixed set of such labels) based off of its arity and orderedness. Assignments are made consistently across the entire graph, e.g., *every* instance of the function MASS across *both* the base and target would be assigned to same generic replacement label. This assignment means that the original label is not used in the matching process, which allows AMN to generalize to symbols it has never seen before.

The label graph is not sufficient to produce representations that can be used for the matching process, as it represents a node by only the label-based features of its dependencies; an issue known as the *type-token distinction* [38, 39]. To contend with this, a signature graph is constructed that allows nodes to be represented by their object identities. To construct the signature graph, AMN replaces each distinct entity with a unique identifier (drawn from a fixed set of possible identifiers). It then assigns each function / predicate a new label based on arity and orderedness. Unlike with the label graph, two differently labeled symbols would be given the same label if they have the same properties.

As all input graphs will be DAGs, AMN uses two separate DAG LSTMs [40] to embed the nodes of the label and signature graphs (equations detailed in Appendix 7.1.1). Each node embedding is computed as a function of its complete set of dependencies in the original graph. In the example in Figure 3, the embedding for GREATER would be a function of the embeddings for both MASS nodes and the two entities nucleus and electron. The set of label embeddings is written as $L_V = \{l_v : v \in V\}$ and the set of signature embeddings is written as $S_V = \{s_v : v \in V\}$. Before passing these

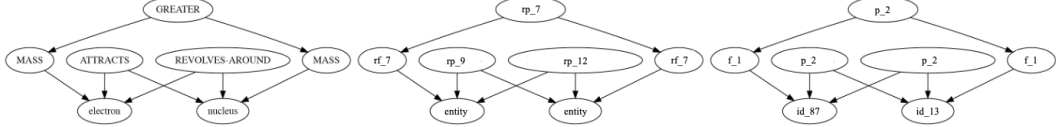


Figure 3: Original graph (left), its label graph (middle), and its signature graph (right)

embeddings to the next step, each element of S_V is scaled to unit length, i.e. each s_v becomes $s_v / \|s_v\|$. Intuitively, this gives our network an efficiently checkable criterion for asserting whether or not two nodes are likely to be equal, i.e., when the dot product of two signature embeddings is 1.

Correspondence Encoder-Decoder: The graph embedding procedure yields two sets of node embeddings (label and signature embeddings) for the base and target. We utilize the set of embedding pairs for each node of V_B and V_T , i.e., $\hat{V}_B = \{\langle l_v, s_v \rangle : v \in V_B\}$ and $\hat{V}_T = \{\langle l_v, s_v \rangle : v \in V_T\}$, with l_v the label embedding of node v taken from L_V and s_v the signature embedding of node v taken from S_V . From \hat{V}_B and \hat{V}_T we define the unprocessed correspondences $\mathcal{C}^{(0)}$ to be

$$\mathcal{C}^{(0)} = \{\langle [l_b; l_t; s_b; s_t], s_b, s_t \rangle : (\langle l_b, s_b \rangle, \langle l_t, s_t \rangle) \in \hat{V}_B \times \hat{V}_T, \|l_b - l_t\| \leq \epsilon\}$$

where $[\cdot; \cdot]$ denotes vector concatenation and ϵ is considered the tiered-identicality threshold that governs how much deviation the embeddings of two nodes may have in order to be considered for correspondence (in this work, we set $\epsilon = 1e-5$). The first element of each correspondence in $\mathcal{C}^{(0)}$, i.e., $h_c = [l_b; l_t; s_b; s_t]$, is passed through the N -layered Transformer encoder (equations detailed in Appendix 7.1.3). This produces a set of encoded correspondences as $\mathcal{E} = \{\langle h_c^{(N)}, s_b, s_t \rangle \in \mathcal{C}^{(N)}\}$.

The objective of the Transformer decoder (equations detailed in Appendix 7.1.3) is to select some subset of the set of correspondences that produces the best analogical match (see Figure 4). The layers of attention-based transformations are performed on only the initial elements of each tuple, i.e., h_d in $\langle h_d, s_b, s_t \rangle$. We let \mathcal{D}_t be the processed set of all selected correspondences (after the N attention layers) and \mathcal{O}_t be the set of all remaining correspondences at timestep t (with $\mathcal{D}_0 = \{\text{START-TOK}\}$ and $\mathcal{O}_0 = \mathcal{E} \cup \{\text{END-TOK}\}$). The decoder generates compatibility scores α_{od} between each pair of elements, i.e., $\langle o, d \rangle \in \mathcal{O}_t \times \mathcal{D}_t$. These are combined with the signature embedding similarities to produce a final compatibility score π_{od} as follows

$$\pi_{od} = \text{FFN}([\tanh \alpha_{od}; s_{b_o}^\top s_{b_d}; s_{t_o}^\top s_{t_d}])$$

where FFN is a two layer feed-forward network with ELU activations. Recall that the signature components, i.e. s_b and s_t , were scaled to unit length. Thus, we would expect closeness in the original graph to be reflected by dot-product similarity and identicality to be indicated by a maximum value dot-product, i.e. $s_{b_o}^\top s_{b_d} = 1$ or $s_{t_o}^\top s_{t_d} = 1$. Once each pair has been scored, AMN selects an element of \mathcal{O}_t to be added to \mathcal{D}_{t+1} . For each $o \in \mathcal{O}_t$, we compute its value to be

$$v_o = \text{FFN}([\max_d \pi_{od}; \min_d \pi_{od}; \sum_d \frac{\pi_{od}}{|\mathcal{D}_t|}])$$

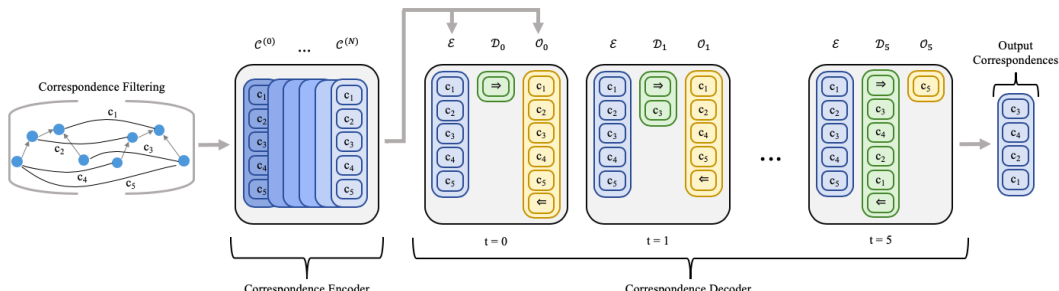


Figure 4: The correspondence selection process, where \Rightarrow and \Leftarrow are the start and stop tokens, \mathcal{E} is the set of encoded correspondences, \mathcal{D}_t is the set of selected correspondences, and \mathcal{O}_t is all remaining correspondences.

where FFN is a two layer feed-forward network with ELU activations. A softmax turns these scores into a probability distribution and the most probable element is added to \mathcal{D}_{t+1} . The use of maximum, minimum, and average lets the network to capture both individual and aggregate evidence. Individual evidence is given by a pairwise interaction between two correspondences (e.g., two correspondences that together violate the one-to-one constraint). Conversely, aggregate evidence is given by the interaction of a correspondence with everything selected thus far (e.g., a correspondence needed for several parallel connectivity constraints). When END-TOK is selected, the set of correspondences M returned is the set of node pairs from V_B and V_T associated with elements in \mathcal{D} .

Candidate Inference Encoder-Decoder: The output of the correspondence selector is a set of correspondences M . The candidate inferences associated with M are drawn from the nodes of the base graph V_B that were *not* used in M . Let V_{in} and V_{out} be the subsets of V_B that were and were not used in M . We first extract all signature embeddings for both sets, i.e., $\mathcal{S}_{in} = \{s_b : b \in V_{in}\}$ and $\mathcal{S}_{out} = \{s_b : b \in V_{out}\}$. Like with the correspondence selector, \mathcal{S}_{in} is processed with a Transformer encoder and we define the encoded comparison set from the Transformer’s N -th layer, i.e. $\mathcal{E} = \mathcal{S}_{in}^{(N)}$.

The Transformer decoder will select elements from \mathcal{S}_{out} to return. As before, we let \mathcal{D}_t be the processed set of all selected elements from \mathcal{S}_{out} (after the N attention layers and with $\mathcal{E} = \mathcal{S}_{in}^{(N)}$ being the encoded set of elements compared against) and \mathcal{O}_t be the set of all remaining elements from \mathcal{S}_{out} at timestep t . The compatibility scores generated by the decoder are given by α_{od} , and are computed between each pair of elements, i.e., $\langle o, d \rangle \in \mathcal{O}_t \times \mathcal{D}_t$. Unlike with the correspondence encoder-decoder there are no other values to combine these scores with, so they are used directly to compute a value v_o for each element of \mathcal{O}_t . In this work, candidate inferences are determined by an individual pairwise relationship; namely, they include any node that had a dependency in M or an ancestor in the set of candidate inferences. Thus, we use a pairwise interaction to determine the value for a potential candidate inference node o , with $v_o = \max_d \alpha_{od}$. Like with the correspondence encoder-decoder, a softmax is used to generate a probability distribution and the most probable element is added to \mathcal{D}_{t+1} . Once a special end token is selected, the decoding procedure stops and returns the set of nodes associated with elements in \mathcal{D} .

Loss Function: As both the correspondence and candidate inference components use a softmax, the loss function is categorical cross entropy. Teacher forcing is used to guide the decoder to select the correct choices during training. The losses for both the correspondence and candidate inference components are summed together to produce the final loss which is minimized with Adam [41].

4.2 Model Scoring

Structural Match Scoring: We define M to be the output correspondences. In order to avoid counting erroneous correspondence predictions towards the score of M , we first identify all correspondences that are either degenerate or violate the constraints of SMT. Degenerate correspondences are correspondences between constants that have no higher-order structural support in M (i.e., neither one has a parent that participates in a correspondence in M). To determine whether a correspondence $\langle b, t \rangle$ violates SMT constraints, we check whether the subgraphs of the base and target rooted at b and t satisfy the one-to-one matching, parallel connectivity, and tiered identicality constraints (see Section 3). The check can be computed in time linear with the size of the corresponding subgraphs. Let the valid subset of the analogical matching be M_{val} . A correspondence m is considered a *root correspondence* if there does not exist another correspondence m' such that $m' \in M_{val}$ and a node in m' is an ancestor of a node in m . We define $M_{root} \subseteq M_{val}$ to be the set of all such root correspondences. For a correspondence $m = \langle b, t \rangle$ in M_{val} , its score $s(m)$ is given as the size of the subgraph rooted at b in the base. The structural match score for M is then sum of scores for all correspondences in M_{root} , i.e., $s(M) = \sum_{m \in M_{root}} s(m)$. This repeatedly counts nodes that appear in the dependencies of multiple correspondences. This behavior is intentional and leads to higher scores for more interconnected matchings, in keeping with the systematicity preference of SMT.

Structural Evaluation Maximization: Dynamically assigning labels to each example allows AMN to handle never-before-seen symbols, but its inherent randomness can lead to significant variability in terms of outputs. AMN combats this by running each test problem r times and returning the predicted match M that maximizes the structural evaluation score, i.e., $M = \arg \max_{M_r} s(M_r)$. Re-running multiple times smooths over the randomness of assignment in the label and signature

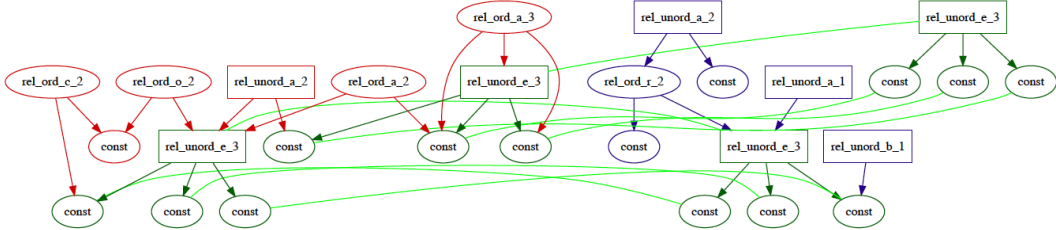


Figure 5: Synthetic example with a base (red), target (blue), and shared subgraphs (green)

graphs without incurring much overhead, since the quality of a match can be checked efficiently. It also gives AMN its preference for systematicity by choosing the mapping that maximizes structural evaluation score. Notably, AMN does not attempt to alter or correct the mapping it chooses this way, so unlike systems like SME, the mapping it returns can include constraint violations.

5 Experiments

5.1 Data Generation and Training

A single example consists of a base graph, a target graph, a set of correspondences between the base and target, and a set of nodes from the base to be considered as candidate inferences. To generate a synthetic example for training, we first generate a set of random graphs C , which will form the basis for the correspondences. Next, we construct the base B by further generating graphs around C . Likewise, for the target T we also build another set of graphs around the C . The graphs of C are then used to form the correspondences between the base and target. Any element in B that is an ancestor of a node from C or a descendent of such an ancestor is considered a candidate inference. Figure 5 provides an example. In the figure, the dark green nodes indicate the initial random graphs C after being copied into the base and target. The red and blue nodes show the graphs built around the initial graphs for B and T . The light green edges indicate the gold set of correspondences generated from C . During training, each generated example was turned into a batch of inputs by repeatedly running the encoding procedure (which dynamically assigns node labels) over the original base and target.

5.2 Experimental Domains

Though all training was done with synthetic data, we evaluated the effectiveness of AMN on both synthetic data and data used in previous analogy experiments. The corpus of previous analogy examples was taken from the public release of SME¹. Importantly, AMN was *not* trained on the corpus of existing analogy examples (AMN never learned from a real-world analogy example). In fact, there was *no* overlap between the symbols used in that corpus and the symbols used for the synthetic data. We briefly describe each of the domains AMN was evaluated on below (though a more detailed description of each domain can be found in [13]). Examples of AMN’s output for each domain can be found in Appendix 7.3.

1. *Synthetic*: this domain consisted of 1000 examples generated with the same parameters as the training data (useful as a sanity check for AMN’s performance).
2. *Visual Oddity*: this problem setting was initially proposed to explore cultural differences to geometric reasoning in [42]. The work of [43] modeled the findings of the original experiment computationally with qualitative visual representations and analogy. We extracted 3405 analogical comparisons from the computational experiment.
3. *Moral Decision Making*: this domain was taken from the work of [44], who introduced a computational model of moral decision making that used SME to reason through moral dilemmas. From the works of [44, 45], we extracted 420 analogical comparisons.
4. *Geometric Analogies*: this domain originated from one of the first computational analogy experiments [46]. Each problem was an incomplete analogy of the form $A : B :: C : ?$, where each of

¹<http://www.qrg.northwestern.edu/software/sme4/index.html>

Table 1: AMN experimental results

(a) AMN correspondence prediction results in terms of performance ratio (left), solution type rate (middle, \uparrow better), and error rate (right, \downarrow better)

Domain	r	Struct. Perf.	Larger	Equiv.	Err. Free	1-to-1 Err.	PC Err.	Degen. Err.
Synthetic	1	0.712	0.001	0.374	0.414	0.010	0.103	0.004
Synthetic	16	0.955	0.002	0.792	0.810	0.009	0.018	0.000
Oddity	1	0.745	0.063	0.403	0.486	0.173	0.190	0.000
Oddity	16	0.952	0.076	0.518	0.611	0.139	0.092	0.000
Moral DM	1	0.581	0.012	0.023	0.112	0.000	0.188	0.005
Moral DM	16	0.955	0.136	0.250	0.514	0.000	0.035	0.001
Geometric	1	0.878	0.068	0.550	0.684	0.043	0.105	0.000
Geometric	16	1.035	0.068	0.736	0.814	0.036	0.033	0.000

(b) AMN candidate inference prediction results

Domain	r	Avg. Cand. Inf. F1	Avg. Cand. Inf. Prec.	Avg. Cand. Inf. Rec.
Synthetic	16	0.749	0.818	0.719
Oddity	16	0.887	0.995	0.861
Moral DM	16	0.797	0.826	0.778
Geometric	16	0.902	0.958	0.904

A , B , and C were manually encoded geometric figures and the goal was to select the figure that best completed the analogy from an encoded set of possible answers. While in the original work all figures had to be manually encoded, in [47, 48] it was shown that the analogy problems could be solved with structure-mapping over automatic encodings (produced by the CogSketch system [49]). From that work we extracted 866 analogies.

5.3 Results and Discussion

Table 1a shows the results for AMN across different values of r , where r denotes the re-run hyper-parameter detailed in Section 4.2. When evaluating on the synthetic data, the comparison set of correspondences was given by the data generator; whereas when evaluating on the three other analogy domains, the comparison set of correspondences was given by the output of SME. It is important to note that we are using SME as our stand-in for SMT (as it is the most widely accepted computational model of SMT). Thus, we do *not* want significantly different results from SME in the correspondence selection experiments (e.g., substantially higher or lower structural evaluation scores).

In the Struct. Perf. column, the numbers reflect the average across examples of the structural evaluation score of AMN divided by that of the comparison correspondence sets. For the other columns of Table 1a, the numbers represent average fractions of examples or correspondences (e.g., 0.684 should be interpreted as 68.4%). Candidate inference prediction performance was measured relative to the set of correspondences AMN generated. That is, all liberal candidate inferences (see Section 3) were computed from the *predicted* set of correspondences, and treated as the true positive predictions for computing Table 1b.

Analysis: The left side of Table 1a shows the average ratio of AMN’s performance (labeled Struct. Perf.), as measured by structural evaluation score, against the comparison method’s performance (i.e., data generator correspondences or SME) across domains. As can be seen, AMN was between 95-104% of SME’s performance in terms of structural evaluation score on the three preexisting domains, which indicates that it was finding similar structural matches. Again, we note that a higher structural evaluation score does *not* necessarily indicate a “better” match, as our goal is to show AMN conforms to SMT’s predictions.

The middle of Table 1a gives us the best sense of how well AMN modeled SMT. We observe AMN’s performance in terms of the proportion of *larger*, *equivalent*, and *error-free* matches it produces (labeled Larger, Equiv., and Err. Free, respectively). Error-free matches do not contain degenerate correspondences or SMT constraint violations, whereas equivalent and larger matches are both error-free and have the same / larger structural evaluation score as compared to gold set of correspondences.

The Equiv. column provides the best indication that AMN could model SMT. It shows that over 50% of AMN’s outputs were SMT-satisfying, error-free analogical matches with the *exact same* structural score as SME (the lead computational model of SMT) in two of the three previous analogy domains.

The right side of Table 1a shows the frequency of the different types of errors, including violations of the one-to-one and parallel connectivity constraints, and degenerate correspondences (labeled 1-to-1 Err., PC Err., and Degen. Err., respectively). It shows that AMN tended to have fairly low error rates across domains (except for Visual Oddity). Importantly, degenerate correspondences were not an issue for any domain, which is significant because it verifies that AMN leveraged higher-order relational structure when generating matches.

Table 1b shows that AMN was fairly effective in predicting candidate inferences. Interestingly, the average F1 score for the Geometric Analogies domain was lower than both the average precision and recall. This indicates that problems with lower recall tended to have higher precision and vice versa. The high precision scores for both Visual Oddity and Geometric Analogies domain indicate that AMN could capture the notion structural support when determining candidate inferences.

6 Conclusions & Future Work

In this paper, we introduced the Analogical Matching Network, an end-to-end neural approach that learned to produce analogies consistent with Structure-Mapping Theory. Despite being trained on completely synthetic data, AMN was capable of performing well on a varied set of analogies drawn from previous work involving analogical reasoning. AMN demonstrated renaming invariance, structural sensitivity, and the ability to find solutions in a combinatorial search space, all of which are key properties of symbolic reasoners and are known to be important to human reasoning.

These properties of AMN point the way to further integration between the fields of deep learning, symbolic reasoning, and cognitive science. For example, renaming invariance and structural sensitivity could be useful in designing neural heuristics for symbolic reasoners. The mappings provided by AMN could serve as higher-order relations for other neural systems to exploit during learning. And although AMN takes a very different approach than prior connectionist models of analogy, comparisons between the two could produce new insights about what properties are essential for analogy and how they might be implemented in the human mind. More work is needed to explore the boundary between deep learning and analogical reasoning and determine the prospects for future collaborations between the two fields.

References

- [1] Dedre Gentner. Why we’re so smart. *Language in mind: Advances in the study of language and thought*, 195235, 2003.
- [2] Douglas R Hofstadter. Analogy as the core of cognition. *The analogical mind: Perspectives from cognitive science*, pages 499–538, 2001.
- [3] Douglas Hofstadter. *Fluid concepts and creative analogies: Computer models of the fundamental mechanisms of thought*. Basic books, 1995.
- [4] Eyal Sagi, Dedre Gentner, and Andrew Lovett. What difference reveals about similarity. *Cognitive science*, 36(6):1019–1050, 2012.
- [5] Dedre Gentner, Sarah Brem, Ronald W Ferguson, Arthur B Markman, Bjorn B Levidow, Phillip Wolff, and Kenneth D Forbus. Analogical reasoning and conceptual change: A case study of johannes kepler. *The journal of the learning sciences*, 6(1):3–40, 1997.
- [6] Keith J Holyoak, Ellen N Junn, and Dorrit O Billman. Development of analogical problem-solving skill. *Child development*, pages 2042–2055, 1984.
- [7] Laura R Novick. Analogical transfer, problem similarity, and expertise. *Journal of Experimental Psychology: Learning, memory, and cognition*, 14(3):510, 1988.
- [8] Mary L Gick and Keith J Holyoak. Schema induction and analogical transfer. 1983.
- [9] Melanie Mitchell. *Analogy-making as perception: A computer model*. 1993.

[10] David J Chalmers, Robert M French, and Douglas R Hofstadter. High-level perception, representation, and analogy: A critique of artificial intelligence methodology. *Journal of Experimental & Theoretical Artificial Intelligence*, 4(3):185–211, 1992.

[11] Dedre Gentner. Structure-mapping: A theoretical framework for analogy. *Cognitive science*, 7(2):155–170, 1983.

[12] Keith J Holyoak, Keith James Holyoak, and Paul Thagard. *Mental leaps: Analogy in creative thought*. 1996.

[13] Kenneth D Forbus, Ronald W Ferguson, Andrew Lovett, and Dedre Gentner. Extending sme to handle large-scale cognitive modeling. *Cognitive Science*, 41(5):1152–1201, 2017.

[14] Keith J Holyoak and Paul Thagard. Analogical mapping by constraint satisfaction. *Cognitive science*, 13(3):295–355, 1989.

[15] Tony Vealeli Diarmuid O'Donoghue and Mark Keane. Computability as a limiting cognitive constraint: Complexity concerns in metaphor comprehension about which cognitive linguists should be aware. In *Cultural, Psychological and Typological Issues in Cognitive Linguistics: Selected papers of the bi-annual ICLA meeting in Albuquerque, July 1995*, volume 152, page 129. John Benjamins Publishing, 1999.

[16] Tony Veale and Mark T Keane. The competence of sub-optimal theories of structure mapping on hard analogies. In *IJCAI (1)*, pages 232–237, 1997.

[17] Danilo Ribeiro, Thomas Hinrichs, Maxwell Crouse, Kenneth Forbus, Maria Chang, and Michael Witbrock. Predicting state changes in procedural text using analogical question answering. 2013.

[18] Maxwell Crouse, Clifton McFate, and Kenneth Forbus. Learning from unannotated qa pairs to analogically disambiguate and answer questions. In *Thirty-Second AAAI Conference on Artificial Intelligence*, 2018.

[19] Kezhen Chen, Irina Rabkina, Matthew D McLure, and Kenneth D Forbus. Human-like sketch object recognition via analogical learning. In *Proceedings of the AAAI Conference on Artificial Intelligence*, volume 33, pages 1336–1343, 2019.

[20] Kezhen Chen and Kenneth Forbus. Action recognition from skeleton data via analogical generalization over qualitative representations. In *Thirty-Second AAAI Conference on Artificial Intelligence*, 2018.

[21] Matthew Klenk, Kenneth D Forbus, Emmett Tomai, Hyeonkyeong Kim, and Brian Kyckelhahn. Solving everyday physical reasoning problems by analogy using sketches. In *AAAI Conference on Artificial Intelligence*, 2005.

[22] Scott Friedman and Kenneth Forbus. An integrated systems approach to explanation-based conceptual change. In *Twenty-Fourth AAAI Conference on Artificial Intelligence*, 2010.

[23] Dedre Gentner and Arthur B Markman. Analogy–watershed or waterloo? structural alignment and the development of connectionist models of analogy. In *Advances in neural information processing systems*, pages 855–862, 1993.

[24] Graeme S Halford, William H Wilson, Jian Guo, Ross W Gayler, Janet Wiles, and JEM Stewart. Connectionist implications for processing capacity limitations in analogies.

[25] Chris Eliasmith and Paul Thagard. Integrating structure and meaning: A distributed model of analogical mapping. *Cognitive Science*, 25(2):245–286, 2001.

[26] John E Hummel and Keith J Holyoak. Distributed representations of structure: A theory of analogical access and mapping. *Psychological review*, 104(3):427, 1997.

[27] John E Hummel and Keith J Holyoak. Relational reasoning in a neurally plausible cognitive architecture: An overview of the lisa project. *Current Directions in Psychological Science*, 14(3):153–157, 2005.

[28] Dedre Gentner. Analogy. *A companion to cognitive science*, pages 107–113, 2017.

[29] Felix Hill, Adam Santoro, David GT Barrett, Ari S Morcos, and Timothy Lillicrap. Learning to make analogies by contrasting abstract relational structure. *International Conference on Learning Representations*, 2019.

[30] Chi Zhang, Feng Gao, Baoxiong Jia, Yixin Zhu, and Song-Chun Zhu. Raven: A dataset for relational and analogical visual reasoning. In *Proceedings of the IEEE Conference on Computer Vision and Pattern Recognition*, pages 5317–5327, 2019.

[31] Tomáš Mikolov, Wen-tau Yih, and Geoffrey Zweig. Linguistic regularities in continuous space word representations. In *Proceedings of the 2013 conference of the north american chapter of the association for computational linguistics: Human language technologies*, pages 746–751, 2013.

[32] Scott E Reed, Yi Zhang, Yuting Zhang, and Honglak Lee. Deep visual analogy-making. In *Advances in neural information processing systems*, pages 1252–1260, 2015.

[33] Brian F Bowdle and Dedre Gentner. Informativity and asymmetry in comparisons. *Cognitive Psychology*, 34(3):244–286, 1997.

[34] Dedre Gentner and Arthur B Markman. Analogy-based reasoning. In *The handbook of brain theory and neural networks*, pages 91–93. MIT Press, 1998.

[35] Ashish Vaswani, Noam Shazeer, Niki Parmar, Jakob Uszkoreit, Llion Jones, Aidan N Gomez, Łukasz Kaiser, and Illia Polosukhin. Attention is all you need. In *Advances in neural information processing systems*, pages 5998–6008, 2017.

[36] Oriol Vinyals, Meire Fortunato, and Navdeep Jaitly. Pointer networks. In *Advances in neural information processing systems*, pages 2692–2700, 2015.

[37] Wouter Kool, Herke Van Hoof, and Max Welling. Attention, learn to solve routing problems! *arXiv preprint arXiv:1803.08475*, 2018.

[38] Daniel Kahneman, Anne Treisman, and Brian J Gibbs. The reviewing of object files: Object-specific integration of information. *Cognitive psychology*, 24(2):175–219, 1992.

[39] Linda Wetzel. Types and tokens. 2006.

[40] Maxwell Crouse, Ibrahim Abdelaziz, Cristina Cornelio, Veronika Thost, Lingfei Wu, Kenneth Forbus, and Achille Fokoue. Improving graph neural network representations of logical formulae with subgraph pooling. *arXiv preprint arXiv:1911.06904*, 2019.

[41] Diederik P Kingma and Jimmy Ba. Adam: A method for stochastic optimization. *arXiv preprint arXiv:1412.6980*, 2014.

[42] Stanislas Dehaene, Véronique Izard, Pierre Pica, and Elizabeth Spelke. Core knowledge of geometry in an amazonian indigene group. *Science*, 311(5759):381–384, 2006.

[43] Andrew Lovett and Kenneth Forbus. Cultural commonalities and differences in spatial problem-solving: A computational analysis. *Cognition*, 121(2):281–287, 2011.

[44] Morteza Dehghani, Emmett Tomai, Ken Forbus, Rumen Iliev, and Matthew Klenk. Moraldm: A computational model of moral decision-making. In *Proceedings of the Annual Meeting of the Cognitive Science Society*, 2008.

[45] Morteza Dehghani, Emmett Tomai, Kenneth D Forbus, and Matthew Klenk. An integrated reasoning approach to moral decision-making. In *AAAI*, pages 1280–1286, 2008.

[46] Thomas G Evans. A program for the solution of a class of geometric-analogy intelligence-test questions. Technical report, AIR FORCE CAMBRIDGE RESEARCH LABS LG HANSCOM FIELD MASS, 1964.

[47] Andrew Lovett, Emmett Tomai, Kenneth Forbus, and Jeffrey Usher. Solving geometric analogy problems through two-stage analogical mapping. *Cognitive science*, 33(7):1192–1231, 2009.

[48] Andrew Lovett and Kenneth Forbus. Modeling multiple strategies for solving geometric analogy problems. In *Proceedings of the Annual Meeting of the Cognitive Science Society*, volume 34, 2012.

[49] Kenneth Forbus, Jeffrey Usher, Andrew Lovett, Kate Lockwood, and Jon Wetzel. Cogsketch: Sketch understanding for cognitive science research and for education. *Topics in Cognitive Science*, 3(4):648–666, 2011.

[50] Kai Sheng Tai, Richard Socher, and Christopher D Manning. Improved semantic representations from tree-structured long short-term memory networks. In *Proceedings of the 53rd Annual Meeting of the Association for Computational Linguistics and the 7th International Joint Conference on Natural Language Processing (Volume 1: Long Papers)*, pages 1556–1566, 2015.

- [51] Jimmy Lei Ba, Jamie Ryan Kiros, and Geoffrey E Hinton. Layer normalization. *arXiv preprint arXiv:1607.06450*, 2016.
- [52] Djork-Arné Clevert, Thomas Unterthiner, and Sepp Hochreiter. Fast and accurate deep network learning by exponential linear units (elus). *arXiv preprint arXiv:1511.07289*, 2015.

7 Appendix

7.1 Background

7.1.1 DAG LSTMs

DAG LSTMs extend Tree LSTMs [50] to DAG-structured data. As with Tree LSTMs, DAG LSTMs compute each node embedding as the aggregated information of all their immediate predecessors (the equations for the DAG LSTM are identical to those of the Tree LSTM). The difference between the two is that DAG LSTMs stage the computation of a node’s embedding based on the order given by a topological sort of the input graph. Batching of computations is done by grouping together updates of independent nodes (where two nodes are independent if they are neither ancestors nor predecessors of one another). As in [40], for a node, v , its initial node embedding, s_v , is assigned based on its label and arity. The DAG LSTM then computes the final embedding h_v to be

$$\begin{aligned} i_v &= \sigma(W_i s_v + \sum_{w \in \mathcal{P}(v)} U_i^{(e_{vw})} h_w + b_i) \\ o_v &= \sigma(W_o s_v + \sum_{w \in \mathcal{P}(v)} U_o^{(e_{vw})} h_w + b_o) \\ \hat{c}_v &= \tanh(W_c s_v + \sum_{w \in \mathcal{P}(v)} U_c^{(e_{vw})} h_w + b_c) \\ f_{vw} &= \sigma(W_f s_v + U_f^{(e_{vw})} h_w + b_f) \\ c_v &= i_v \odot \hat{c}_v + \sum_{w \in \mathcal{P}(v)} f_{vw} \odot c_w \\ h_v &= o_v \odot \tanh(c_v) \end{aligned}$$

where \odot is element-wise multiplication, σ is the sigmoid function, \mathcal{P} is the predecessor function that returns the arguments for a node, $U_i^{(e_{vw})}$, $U_o^{(e_{vw})}$, $U_c^{(e_{vw})}$, and $U_f^{(e_{vw})}$ are learned matrices per edge type. i and o represent input and output gates, c and \hat{c} are memory cells, and f is a forget gate.

7.1.2 Multi-Headed Attention

The multi-headed attention (MHA) mechanism of [35] is used in our work to compare correspondences against one another. In this work, MHA is given two inputs, a query vector q and a list of key vectors to compare the query vector against $\langle k_1, \dots, k_n \rangle$. In N -headed attention, N separate attention transformations are computed. For transformation i we have

$$\begin{aligned} \hat{q}_i &= W_i^{(q)} q, k_{ij} = W_i^{(k)} k_j, v_{ij} = W_i^{(v)} k_j \\ w_{ij} &= \frac{\hat{q}_i^\top k_{ij}}{\sqrt{b_q}} \\ \alpha_{ij} &= \frac{\exp(w_{ij})}{\sum_{j'} \exp(w_{ij'})} \\ q_i &= \sum_j \alpha_{ij} \hat{q}_i \end{aligned}$$

where each of $W_i^{(q)}$, $W_i^{(k)}$, and $W_i^{(v)}$ are learned matrices and b_q is the dimensionality of q . The final output vector q' for input q is then given as a combination of its N transformations

$$q' = \sum_{i=1}^N W_i^{(o)} q_i$$

where each $W_i^{(o)}$ is a distinct learned matrix for each i . In implementation, the comparisons of query and key vectors are batched together and performed as efficient matrix multiplications.

7.1.3 Transformer Encoder-Decoder

The Transformer-based encoder-decoder is given two inputs, a comparison set \mathcal{C} and an output set \mathcal{O} . At a high level, \mathcal{C} will be encoded into a new set \mathcal{E} , which will inform a selection process that picks elements of \mathcal{O} to return. The set \mathcal{O} can be the encoded input set (i.e., $\mathcal{O} \equiv \mathcal{E}$ in the context of pointer networks) or it can be some other entirely new set (e.g., an output vocabulary in the context of machine translation).

Encoder: First, the elements of \mathcal{C} , i.e. $h_c \in \mathcal{C}$, are passed through N layers of an attention-based transformation. For element h_c in the i -th layer (i.e., $h_c^{(i-1)}$) this is performed as follows

$$\begin{aligned}\hat{h}_c &= \text{LN}(h_c^{(i-1)} + \text{MHA}_{\mathcal{C}}^{(i)}(h_c^{(i-1)}, \langle h_1^{(i-1)}, \dots, h_j^{(i-1)} \rangle)) \\ h_c^{(i)} &= \text{LN}(\hat{h}_c + \text{FFN}^{(i)}(\hat{h}_c))\end{aligned}$$

where LN denotes the use of layer normalization [51], $\text{MHA}_{\mathcal{C}}^{(i)}$ (Appendix 7.1.2) denotes the use of self multi-headed attention for layer i (i.e., attention between $h_c^{(i)}$ and the other elements of $\mathcal{C}^{(i-1)}$), and $\text{FFN}^{(i)}$ is a two-layer feed-forward neural network with ELU [52] activations. After N layers of processing, the set of encoded inputs \mathcal{E} is given by $\mathcal{E} = \mathcal{C}^{(N)}$

Decoder: With encoded comparison elements \mathcal{E} and a set of potential outputs \mathcal{O} , the objective of the decoder is to use \mathcal{E} to inform the selection of some subset of output options $\mathcal{D} \subseteq \mathcal{O}$ to return. Decoding happens sequentially; at each timestep $t \in \{1, \dots, n\}$ the decoder selects an element from $\mathcal{O} \cup \{\text{END-TOK}\}$ (where END-TOK is a learned triple) to add to \mathcal{D} . If END-TOK is chosen, the decoding procedure stops and \mathcal{D} is returned.

Let \mathcal{D}_t be the set of elements that have been selected by timestep t and \mathcal{O}_t be the remaining unselected elements at timestep t . First, \mathcal{D}_t is processed with an N -layered attention-based transformation. For an element $h_d^{(i-1)}$ this is given by

$$\begin{aligned}\hat{h}_d &= \text{LN}(h_d^{(i-1)} + \text{MHA}_{\mathcal{D}}^{(i)}(h_d^{(i-1)}, \langle h_1^{(i-1)}, \dots, h_j^{(i-1)} \rangle)) \\ \hat{h}_d &= \text{LN}(\hat{h}_d + \text{MHA}_{\mathcal{E}}^{(i)}(\hat{h}_d, \langle h_1^{(i-1)}, \dots, h_l^{(i-1)} \rangle)) \\ h_d^{(i)} &= \text{LN}(\hat{h}_d + \text{FFN}^{(i)}(\hat{h}_d))\end{aligned}$$

where $\text{MHA}_{\mathcal{D}}^{(i)}$ denotes the use of self multi-headed attention, $\text{MHA}_{\mathcal{E}}^{(i)}$ denotes the use of multi-headed attention against elements of \mathcal{E} , and $\text{FFN}^{(i)}$ is a two-layer feed-forward neural network with ELU activations. We will consider the already selected outputs to be the transformed selected outputs, i.e., $\mathcal{D}_t = \mathcal{D}_t^{(N)}$. For a pair, $\langle h_o, h_d \rangle \in \mathcal{O}_t \times \mathcal{D}_t$, we compute their compatibility as α_{od}

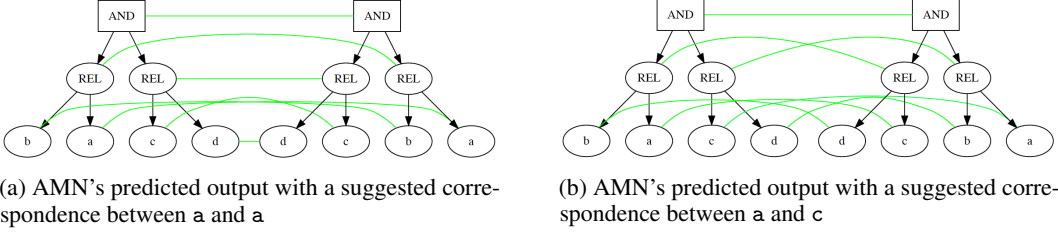
$$\begin{aligned}q_{od} &= W_q h_d^{(n)}, k_{od} = W_k h_o \\ \alpha_{do} &= \frac{q_{od}^\top k_{od}}{\sqrt{b_o}}\end{aligned}$$

where W_q and W_k are learned matrices, b_o is the dimensionality of h_o , and FFN is a two layer feed-forward network with ELU activations. This defines a matrix $H \in \mathbb{R}^{|\mathcal{O}_t| \times |\mathcal{D}_t|}$ of compatibility scores. One can then apply some operation (e.g., max pooling) to produce a vector of values $v_t \in \mathbb{R}^{|\mathcal{O}_t|}$ which can be fed into a softmax to produce a distribution over options from \mathcal{O}_t . The highest probability element δ^* from the distribution is then added to the set of selected outputs, i.e., $\mathcal{D} = \mathcal{D}_t \cup \{\delta^*\}$.

7.2 Extensions to AMN

7.2.1 Suggested Correspondences

The design of AMN is flexible enough to allow for prior knowledge to seed the matching process. Let \mathcal{S} be a set of correspondences that the user specifies should be preferred. To include \mathcal{S} , AMN



(a) AMN's predicted output with a suggested correspondence between a and a
(b) AMN's predicted output with a suggested correspondence between a and c

Figure 6: Suggested correspondences in a self-match involving $\text{AND}(\text{REL}(a, b), \text{REL}(c, d))$

simply modifies the initial set of encoded correspondences \mathcal{C} as follows

$$\check{\mathcal{C}} = \{\langle [l_b; l_t; s_b; s_t], s_b, s_t \rangle \in \hat{\mathcal{C}} : (\|l_b - l_t\| \leq \epsilon) \wedge (\forall b', t'. \langle b, t' \rangle \notin \mathcal{S} \wedge \langle b', t' \rangle \notin \mathcal{S})\}$$

$$\mathcal{C}^{(0)} = \check{\mathcal{C}} \cup \{\langle [l_b; l_t; s_b; s_t], s_b, s_t \rangle : \langle b, t \rangle \in \mathcal{S}\}$$

Informally, $\check{\mathcal{C}}$ denotes the set of all structurally similar correspondences *without* a node that is a part of some correspondence in \mathcal{S} . $\mathcal{C}^{(0)}$ is then $\check{\mathcal{C}}$ combined with the set of suggested correspondences \mathcal{S} . Figure 6 shows how suggested correspondences can change the output of AMN. We refer to them as suggested correspondences because AMN may not use them in its final output (for instance, if the correspondences are incompatible with parallel connectivity).

7.3 AMN Example Outputs

For the outputs from the non-synthetic domains (all but the first figure), only small subgraphs of the original graphs are shown (the original graphs were too large to be displayed)

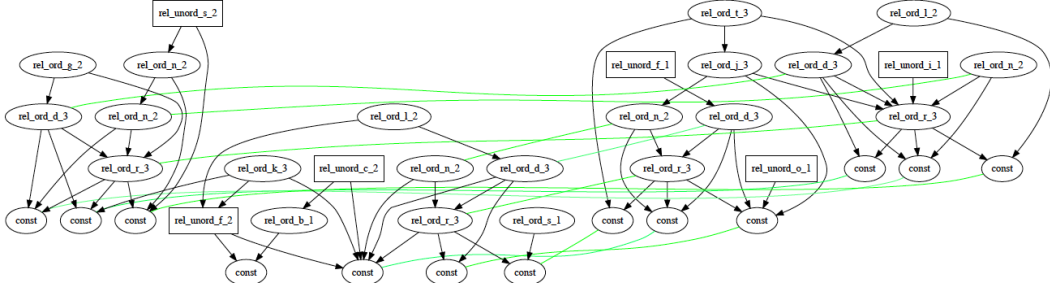


Figure 7: AMN output for an example from the Synthetic domain

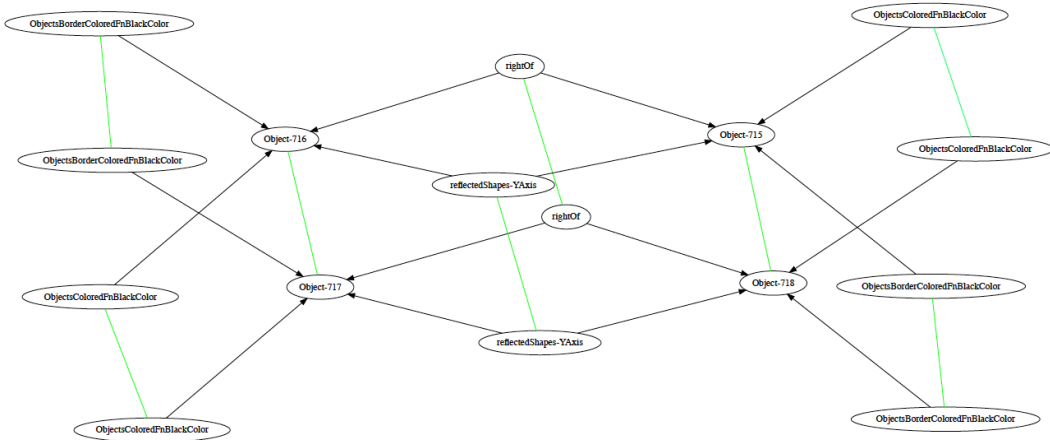


Figure 8: AMN output for an example from the Visual Oddity domain

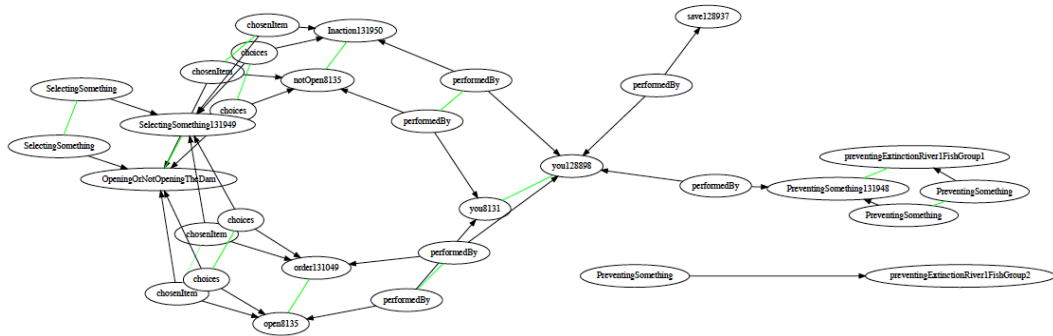


Figure 9: AMN output for an example from the Moral Decision Making domain

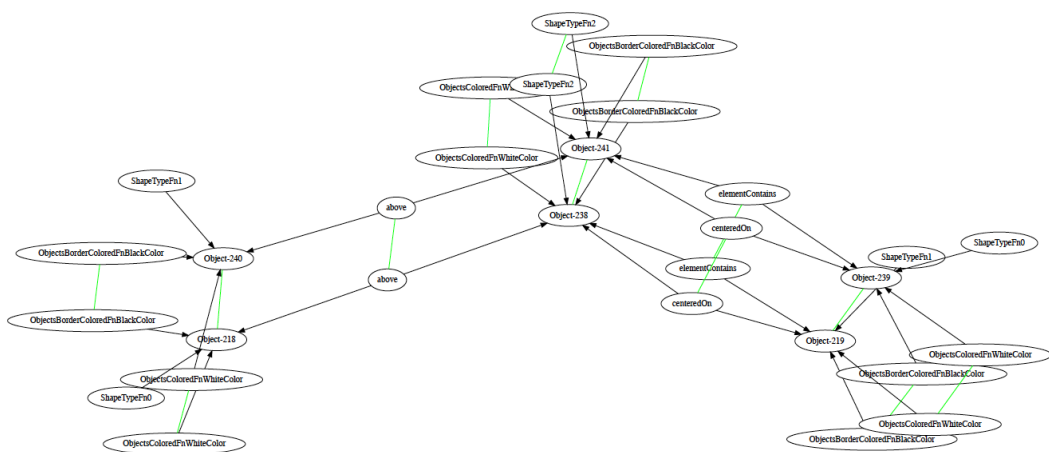


Figure 10: AMN output for an example from the Geometric Analogies domain